

Dynamics and synchronization of neural models with memristive membranes under energy coupling

Jingyue Wan(万婧玥), Fuqiang Wu(吴富强), Jun Ma(马军), and Wenshuai Wang(汪文帅)

Citation: Chin. Phys. B, 2024, 33 (**5**): 050504. DOI: 10.1088/1674-1056/ad1dcc
Journal homepage: http://cpb.iphy.ac.cn; http://iopscience.iop.org/cpb

What follows is a list of articles you may be interested in

Dynamics analysis and cryptographic implementation of a fractional-order memristive cellular neural network model

Xinwei Zhou(周新卫), Donghua Jiang(蒋东华), Jean De Dieu Nkapkop, Musheer Ahmad, Jules Tagne Fossi, Nestor Tsafack, and Jianhua Wu(吴建华)
Chin. Phys. B, 2024, 33 (**4**): 040506. DOI: 10.1088/1674-1056/ad03dd

Coexistence behavior of asymmetric attractors in hyperbolic-type memristive Hopfield neural network and its application in image encryption

Xiaoxia Li(李晓霞), Qianqian He(何倩倩), Tianyi Yu(余天意),Zhuang Cai(才壮), and Guizhi Xu(徐桂芝)
Chin. Phys. B, 2024, 33 (**3**): 030505. DOI: 10.1088/1674-1056/acf281

Multiple mixed state variable incremental integration for reconstructing extreme multistability in a novel memristive hyperchaotic jerk system with multiple cubic nonlinearity

Meng-Jiao Wang(王梦蛟) and Lingfang Gu(辜玲芳)
Chin. Phys. B, 2024, 33 (**2**): 020504. DOI: 10.1088/1674-1056/acddd0

Bipolar-growth multi-wing attractors and diverse coexisting attractors in a new memristive chaotic system

Wang-Peng Huang(黄旺鹏) and Qiang Lai(赖强)
Chin. Phys. B, 2023, 32 (**10**): 100504. DOI: 10.1088/1674-1056/ace1d9

Dynamical analysis, geometric control and digital hardware implementation of a complex-valued laser system with a locally active memristor

Yi-Qun Li(李逸群), Jian Liu(刘坚), Chun-Biao Li(李春彪), Zhi-Feng Hao(郝志峰), and Xiao-Tong Zhang(张晓彤)
Chin. Phys. B, 2023, 32 (**8**): 080503. DOI: 10.1088/1674-1056/acd68b

---

Dynamics and synchronization of neural models with memristive membranes under energy coupling

Jingyue Wan(万婧玥)[1], Fuqiang Wu(吴富强)[1,2,†], Jun Ma(马军)[3], and Wenshuai Wang(汪文帅)[1,2]

[1] *School of Mathematics and Statistics, Ningxia University, Yinchuan* 750021, *China*
[2] *Ningxia Basic Science Research Center of Mathematics, Ningxia University, Yinchuan* 750021, *China*
[3] *Department of Physics, Lanzhou University of Technology, Lanzhou* 730050, *China*

(Received 6 December 2023; revised manuscript received 29 December 2023; accepted manuscript online 12 January 2024)

Dynamical modeling of neural systems plays an important role in explaining and predicting some features of biophysical mechanisms. The electrophysiological environment inside and outside of the nerve cell is different. Due to the continuous and periodical properties of electromagnetic fields in the cell during its operation, electronic components involving two capacitors and a memristor are effective in mimicking these physical features. In this paper, a neural circuit is reconstructed by two capacitors connected by a memristor with periodical mem-conductance. It is found that the memristive neural circuit can present abundant firing patterns without stimulus. The Hamilton energy function is deduced using the Helmholtz theorem. Further, a neuronal network consisting of memristive neurons is proposed by introducing energy coupling. The controllability and flexibility of parameters give the model the ability to describe the dynamics and synchronization behavior of the system.

Keywords: memristor, neuronal model, energy, synchronization

PACS: 05.45.Pq, 05.45.Xt, 05.45.Gg **DOI:** 10.1088/1674-1056/ad1dcc

1. Introduction

Activities in biological systems cannot work without energy.[1] The generation of electrical activities in a neural system composed of neurons and synapses is energetically a costly process.[2,3] The metabolic energy is used to maintain the signaling activities of neurons. Many neurons in the brain present extremely complicated firing patterns, including spiking, bursting, and chaotic firing.[4–6] Neuron models have been proposed to reproduce the dynamical firing patterns of real neurons, but it is difficult to characterize the energy required to maintain and transmit these electrical activities.

In recent years, several investigations have been reported that have tried to solve the energy function of neural systems. The neuronal model is constructed by considering membrane features involving the ionic channel effect.[7] The membrane mechanism is associated with an action potential. The sampled time series from the membrane are obtained using patch clamp technology. Based on these biophysical essences, many interesting neural models can describe a relationship between the observed sampling data and biophysical mechanisms. Indeed, biological neurons are regarded as a variety of electric components, such as memristor.[8–13] The neural circuit with abundant functions and behavior is reconstructed by connecting with different electric components.[14–21] Indeed, the firing behavior of a neuron is related to the gradient distribution of an electromagnetic field, induced by exchanging and transporting intracellular and extracellular ions with concentration diversity. Based on the biophysical motivation, a kind of neural model with electromagnetic effects has been proposed and investigated in recent years.[10,21–24] According to a non-smooth feedback strategy, a Filippov hybrid neuron model with electromagnetic induction can show sliding mode dynamics and coexisting attractors.[25] A Hindmarsh–Rose neuron model is improved by introducing magnetic flux and electric field variables, and the model has abundant dynamics and is applied in image encryption.[26] Neuronal models with electromagnetic induction play a significant role in exploring nonlinear dynamics and biophysical mechanisms.

From an energy perspective, neural models with electromagnetic effects have also been investigated. According to the Helmholtz theorem, relationships between firing patterns and energy are found by using numerical computation methods.[27–32] The energy consumption of the Hindmarsh–Rose neuron during its signaling activity can be evaluated by calculating the energy function.[33] The neural networks based on the different neurons can show collective behavior and functional properties.[34,35] Synchronization behavior in the neuronal network is identified by the energy function.[18,36–39] And desynchronization is found in coupled neurons with energy diversity.[40] Complex firing patterns are triggered in an isolated neuronal model subjected to an external stimulus with higher energy density.[32,41] Collective dynamical behavior is triggered in neuronal networks involving memristive effects, local heterogeneity, and energy flow.[28,42–45]

To downplay inessential details and emphasize critical features,[46] nonlinear oscillators and circuits are proposed to mimic or reproduce neuron-like behavior and functions.[47] From the viewpoint of biophysical science, the neural response

†Corresponding author. E-mail: alexwutian@nxu.edu.cn

© 2024 Chinese Physical Society and IOP Publishing Ltd

to the combined influence of electrical, magnetic, and mechanical fields is inextricably linked to exchange and transportation of ions between intracellular and extracellular compartments. It is demonstrated that a sensor with biocompatible traits detects time-varying magnetic fields generated by action potentials.[48] The modelling of a neural system with electromagnetic induction is necessary to explore and explain neural biophysical mechanisms of the rich and complex emergent behavior. The latest work on memristive circuits can present electrical activities under a periodical external stimulus.[22] However, neural systems without periodical stimulus can also show abundant electrical activities. Thus, the memristive circuit without stimulus is further improved, based on the memristive membrane with periodical ionic exchange. Better abundant dynamical patterns are demonstrated in this model. The Hamilton energy function is deduced using the Helmholtz theorem. Further, we develop a network composed of memristive neurons and coupled with the Hamilton energy function. The signal transmission between neural systems requires energy consumption. The energy function can affect the synchronization behavior in the memristive neural network.

The rest of this paper is organized as follows. In Section 2, the neural circuit involving memristive membranes is proposed. We find an energy function for the neural circuit based on Hamilton's theory. In Section 3, we analyze the dynamical behavior in the single neuronal circuit. Further, synchronization is investigated in a network composed of neural circuits under energy coupling. The conclusion is given in Section 4.

2. Model description and method

2.1. Modelling of memristive neural circuit

To explore the dynamics and complex behavior in neural systems, many mathematical models and physical circuits have been proposed. A neural circuit with memristive membranes was constructed using two capacitors, a memristor, an inductor and a nonlinear resistor. A schematic diagram of a single neuron with memristive membranes and a corresponding neural network is presented in Fig. 1.

Based on Kirchhoff's theorem, the equation of the above circuit in Ref. [22] is described as follows:

$$\begin{cases} C_1\dfrac{\mathrm{d}V_1}{\mathrm{d}t} = I_M(\phi) - I_{NR}, \\ C_2\dfrac{\mathrm{d}V_2}{\mathrm{d}t} = -I_M(\phi) + i_L, \\ L\dfrac{\mathrm{d}i_L}{\mathrm{d}t} = -V_2 - Ri_L. \end{cases} \tag{1}$$

where V_1 and V_2 denote the voltage of two capacitors, and i_L represents the current of an inductor, as shown in Fig. 1(a). Here, C_1, C_2, and L are the two capacitances and the inductance, respectively. In a cell, there are two sides to form a physical field. According to the investigation, the ionic channels of the neural system belong to the memristive system.[8,9,49] Here, $I_M(\phi)$ represents the memristive membrane current. Based on the generalized definition of memristive systems, it is defined as

$$\begin{cases} I_M = M(\phi)(V_2 - V_1),\ M(\phi) = \dfrac{\mathrm{d}q(\phi)}{\mathrm{d}\phi} = \dfrac{1}{\rho}\sin\left(\dfrac{\phi}{\rho V_0 C_2}\right), \\ \dfrac{\mathrm{d}\phi}{\mathrm{d}t} = V_2 - V_1. \end{cases} \tag{2}$$

Here, ϕ is magnetic flux, and $M(\phi)$ is the mem-conductance. The mem-conductance is a periodical function, and it is employed to characterize induced time-varying electromagnetic fields via the continuous and periodical diffusion and exchange of intracellular and extracellular ions. To conveniently compare two memristors with different mem-conductance from Ref. [22] and this paper, let $V_2 - V_1$ be equal to $V = A\cos(2\pi ft)$. By integrating the state variable, the mem-conductance in Ref. [22] is solved as

$$M(\phi) = a + b\frac{A^2}{4\pi^2 f^2}\sin^2(2\pi ft). \tag{3}$$

Meanwhile the mem-conductance in this paper is obtained as

$$M(\phi) = \frac{1}{\rho}\sin\left(\frac{A\sin(2\pi ft)}{2\pi f\rho V_0 C_2}\right). \tag{4}$$

Thus, the mem-conductances of two memristors have different odd and even, as shown in Figs. 1(c) and 1(d). The current via the nonlinear resistor in Ref. [22] is described as

$$I_{NR} = -\frac{1}{\rho}\left(V_1 - \frac{V_1^3}{3V_0^2}\right), \tag{5}$$

where ρ is the resistance, and V_0 is the initial voltage.

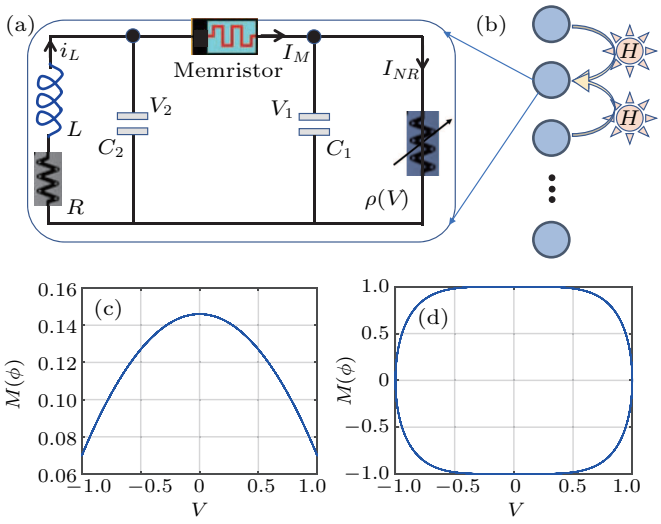


Fig. 1. (a) A schematic diagram of a neural circuit with a memristive connection. A memristor is used to connect two capacitors. The left branch is an inductor in parallel with the capacitors and the right branch is a nonlinear resistor. (b) Schematic blocks of a chain network composed of the memristive neurons. The relationship between the mem-conductance and voltage of the memristor in Ref. [22] (c) and this paper (d) when the input voltage is loaded as $V = A\cos(2.0\pi ft)$. The parameters are selected as $A = 1$, $f = 0.1$, $a = 0.07$, $b = 0.03$, $C_2 = 1$, $V_0 = 1$, and $\rho = 1$.

According to Ref. [22], these physical variables can be changed into dimensionless variables by employing scale transformation as

$$\begin{cases} x=\dfrac{V_1}{V_0}, \quad y=\dfrac{V_2}{V_0}, \quad z=\dfrac{\rho i_L}{V_0}, \quad \varphi=\dfrac{\phi}{\rho V_0 C_2}, \\ \tau=\dfrac{t}{\rho C_2}, \quad \alpha=\dfrac{C_2}{C_1}, \quad \beta=\dfrac{\rho^2 C_2}{L}, \quad \eta=\dfrac{\rho R C_2}{L}. \end{cases} \tag{6}$$

This memristive neuron in Fig. 1(a), using the above scale transformation, is rewritten as

$$\begin{cases} \dfrac{\mathrm{d}x}{\mathrm{d}\tau}=\alpha\left[\sin\varphi(y-x)+x-\dfrac{x^3}{3}\right], \\ \dfrac{\mathrm{d}y}{\mathrm{d}\tau}=\sin\varphi(x-y)+z, \\ \dfrac{\mathrm{d}z}{\mathrm{d}\tau}=-\beta y-\eta z, \\ \dfrac{\mathrm{d}\varphi}{\mathrm{d}\tau}=y-x, \end{cases} \tag{7}$$

where α, β, and η are the parameters selected with suitable values, which can make this model reproduce similar bursting, spiking, and even chaotic patterns. The occurrence of the memristive term is introduced into the neural circuit to describe the time-varying electromagnetic field induced by continuous and periodical diffusion and exchange of intracellular and extracellular ions.

2.2. Modelling of memristive neuronal network

The network of the reciprocally coupled memristive neural model is proposed, and its equation is

$$\begin{cases} \dot{x}_i=\alpha\left[\sin\varphi_i(y_i-x_i)+x_i-\dfrac{x_i^3}{3}\right], \\ \dot{y}_i=\sin\varphi_i(x_i-y_i)+z_i+g_c x_i\sum\limits_j k_{ij}F(H_j-\sigma), \\ \dot{z}_i=-\beta y_i-\eta z_i, \\ \dot{\varphi}_i=y_i-x_i, \end{cases} \tag{8}$$

where x_i, y_i, z_i, and φ_i are the state variables for the ith memristive neuron, respectively, and $I=1,\ldots,N$. Here, k_{ij} is the connectivity matrix, such as a chain in this case, and j is the number of other neurons. Here, g_c is the coupling gain. For the neural circuit, the partial energy of the system is stored in these electric components, including the capacitor, and induced. Meanwhile, the resistor consumes Joule heat. Information transmission between two systems needs physical field energy. Thus, the coupling effect is dependent upon the energy of the system. The physical field energy is described by an equivalent Hamilton energy H. In Eq. (8), $F(H-\sigma)=\tanh(H-\sigma)$ is the nonlinear coupling effect associated with energy. Here, σ is the threshold of the energy level. Specifically, the energy of the system reaches a threshold value, and the electrical activities can be transferred around elements. The parameters are selected as $\alpha=1.0$, $\beta=3.0$, $\eta=1.0$, $\sigma=1.56$, and $g_c=0.0$.

2.3. Energy aspect of isolated model

Inspired by the procedure reported in detail in Refs. [50, 51], the Hamilton energy function of nonlinear oscillators can be obtained. The nonlinear oscillators can be described by

$$\dot{X}=f(X)=f_c(X)+f_d(X), \tag{9}$$

where X is an n-dimensional vector and $f(X)$ is the velocity vector field. Based on a generalized Hamiltonian form, Eq. (9) can be rewritten as

$$\begin{bmatrix} \dot{x} \\ \dot{y} \\ \dot{z} \\ \dot{\varphi} \end{bmatrix}=f_c(x,y,z,\varphi)+f_d(x,y,z,\varphi). \tag{10}$$

Based on the stored energy of the capacitor and inductor and the inner energy of the memristor, the energy function can be expressed as

$$W=\frac{1}{2}C_1V_1^2+\frac{1}{2}C_2V_2^2+\frac{1}{2}Li_L^2+\frac{1}{2}L_MI_M^2, \tag{11}$$

where L_MI_M is regarded as a magnetic flux unit. Based on Eqs. (11) and (6), the energy function is rewritten as

$$\begin{aligned} H &= \frac{1}{C_2V_0^2}W \\ &= \frac{1}{2\alpha}x^2+\frac{1}{2}y^2+\frac{1}{2\beta}z^2+\frac{1}{2}(y-x)\varphi\sin(\varphi). \end{aligned} \tag{12}$$

Further, the time derivative of the energy along a trajectory is written as

$$f_c(x,y,z,\varphi)=\begin{bmatrix} 0 & \alpha & 0 & \alpha \\ -\alpha & 0 & \beta & -1 \\ 0 & -\beta & 0 & 0 \\ -\alpha & 1 & 0 & 0 \end{bmatrix}\cdot\begin{bmatrix} \dfrac{1}{\alpha}x \\ y \\ \dfrac{1}{\beta}z \\ (y-x)\sin(\varphi) \end{bmatrix}. \tag{13}$$

According to Eqs. (10) and (12), the energy derivate is written as

$$\begin{aligned} &f_d(x,y,z,\varphi) \\ &=\begin{bmatrix} \alpha^2\left(1-\dfrac{x^2}{3}-\dfrac{y}{x}\right) & 0 & 0 & 0 \\ 0 & \dfrac{x}{y} & 0 & 0 \\ 0 & 0 & -\beta\eta & 0 \\ 0 & 0 & 0 & 0 \end{bmatrix}\cdot\begin{bmatrix} \dfrac{1}{\alpha}x \\ y \\ \dfrac{1}{\beta}z \\ (y-x)\sin(\varphi) \end{bmatrix}. \end{aligned} \tag{14}$$

According to Ref. [22], the same energy function in Eq. (11) is obtained using the Helmholtz theorem.

2.4. Equilibrium analysis

To obtain the equilibrium points of the system, let $\dot{x} = \dot{y} = \dot{z} = \dot{\varphi} = 0$; then, the equilibrium point $(x^*, y^*, z^*, \varphi^*) = (0, 0, 0, \gamma)$ can be solved, where γ is any real number. It is worth pointing out that the memristive neuron has infinite equilibrium points relative to the initial value of the magnetic variable. To further analyze the stability of the equilibrium points, the Jacobian matrix of the system of equations is solved as

$$J = \begin{pmatrix} 1-\alpha\sin\gamma & \alpha\sin\gamma & 0 & 0 \\ \sin\gamma & -\sin\gamma & 1 & 0 \\ 0 & -\beta & -\eta & 0 \\ -1 & 1 & 0 & 0 \end{pmatrix}. \tag{15}$$

Then, the characteristic polynomial is rewritten as

$$f(\lambda) = \lambda^4 + A_1\lambda^3 + A_2\lambda^2 + A_3\lambda + A_4 = 0, \tag{16}$$

where

$$\begin{cases} A_1 = \alpha\sin\gamma + \sin\gamma + \eta + 1, \\ A_2 = \beta + (\alpha\eta + \eta - 1)\sin\gamma - \eta, \\ A_3 = \beta(\alpha\sin\gamma - 1) - \eta\sin\gamma, \\ A_4 = 0. \end{cases} \tag{17}$$

According to the Routh–Hurwitz stability criterion, when

$$\begin{aligned} \Delta_1 &= \alpha\sin\gamma + \sin\gamma + \eta + 1 > 0, \\ \Delta_2 &= \begin{vmatrix} \alpha\sin\gamma + \sin\gamma + \eta + 1 & \beta(\alpha\sin\gamma - 1) - \eta\sin\gamma \\ 1 & \beta + (\alpha\eta + \eta - 1)\sin\gamma - \eta \end{vmatrix} \\ &= (\alpha+1)(\alpha\eta + \eta - 1)\sin^2\gamma + (\alpha\eta^2 + \eta^2 + \beta - 1)\sin\gamma + \eta(\beta - \eta - 1) + 2\beta > 0, \\ \Delta_3 &= \begin{vmatrix} \alpha\sin\gamma + \sin\gamma + \eta + 1 & \beta(\alpha\sin\gamma - 1) - \eta\sin\gamma & 0 \\ 1 & \beta + (\alpha\eta + \eta - 1)\sin\gamma - \eta & 0 \\ 0 & \alpha\sin\gamma + \sin\gamma + \eta + 1 & \beta(\alpha\sin\gamma - 1) - \eta\sin\gamma \end{vmatrix} \\ &= (\beta(\alpha\sin\gamma - 1) - \eta\sin\gamma)((\alpha+1)(\alpha\eta + \eta - 1)\sin^2\gamma + (\alpha\eta^2 + \eta^2 + \beta - 1)\sin\gamma + \eta(\beta - \eta - 1) + 2\beta) > 0, \end{aligned} \tag{18}$$

the solutions of Eq. (7) are stable. The numerical integrations for the neural circuit and neuronal network are used by the standard fourth-order Runge–Kutta method.[52]

3. Results

3.1. Dynamics and energy of the memristive neural circuit

In this section, we investigate the complex dynamical behavior in a memristive neural circuit by changing two key parameters (α and β). The bifurcation diagram, average firing rate, and average Hamilton energy are depicted in Fig. 2.

Figure 2 shows the comparison of the transition among complex behavior when parameters α and β are controlled separately. The dynamical evolution is obtained by recording the maximum value corresponding to each parameter. The firing pattern transition can be identified by the average firing rate. The energy change is dependent upon firing patterns. The bursting and chaotic dynamics of the neural system have been demonstrated by observing diagrams of the time–voltage series in experiments. Thus, the diagram of the time–voltage series of the memristive neural circuit is numerically described in Fig. 3.

Figure 3 shows that periodical bursting and chaotic firing of the memristive neural circuit are observed when changing the value of α when the other parameters, β and η, are set as 0.71 and 0.01, respectively. It is worth pointing out that the memristive neural circuit is bistable when the initial values are different, as shown in Figs. 3(b) and 3(c) or 3(e) and 3(f). At the origin point, the circuit is eventually in a continuously stable state. To better display the complex dynamical behavior of the model, the bifurcation series diagram of the maxima voltage (x_{peak}) and average energy when changing the parameter α at fixed $\beta = 2.0$, 3.0, 3.5, and 4.0, respectively, are plotted in Fig. 4.

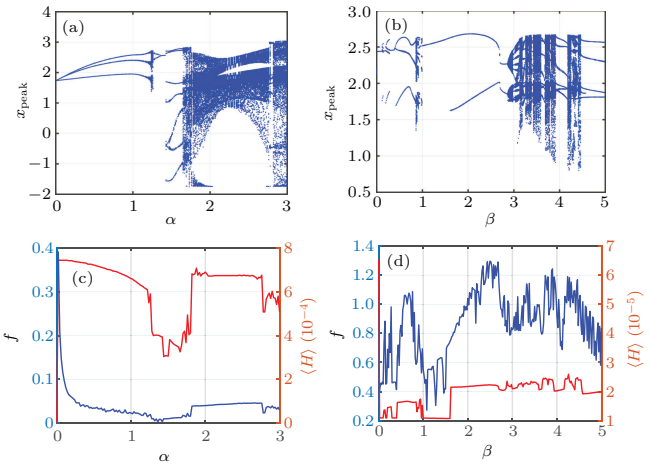


Fig. 2. (a) and (c) The bifurcation diagram and energy diagram for the memristive neural system with the increasing parameter α while fixed at $\beta = 0.71$. (b) and (d) The bifurcation diagram and energy diagram for the memristive neural system with the increasing parameter β while fixed at $\alpha = 3$, respectively.

Figure 4 shows that the memristive neural circuit can present abundant dynamical behavior when increasing the

value of α under the four different β values. The average frequency and energy changes are also relatively gentle when the model belongs to periodical activity. Meanwhile, the average frequency and energy changes are shaking in intensity when the chaotic state is triggered in the model without external stimulus.

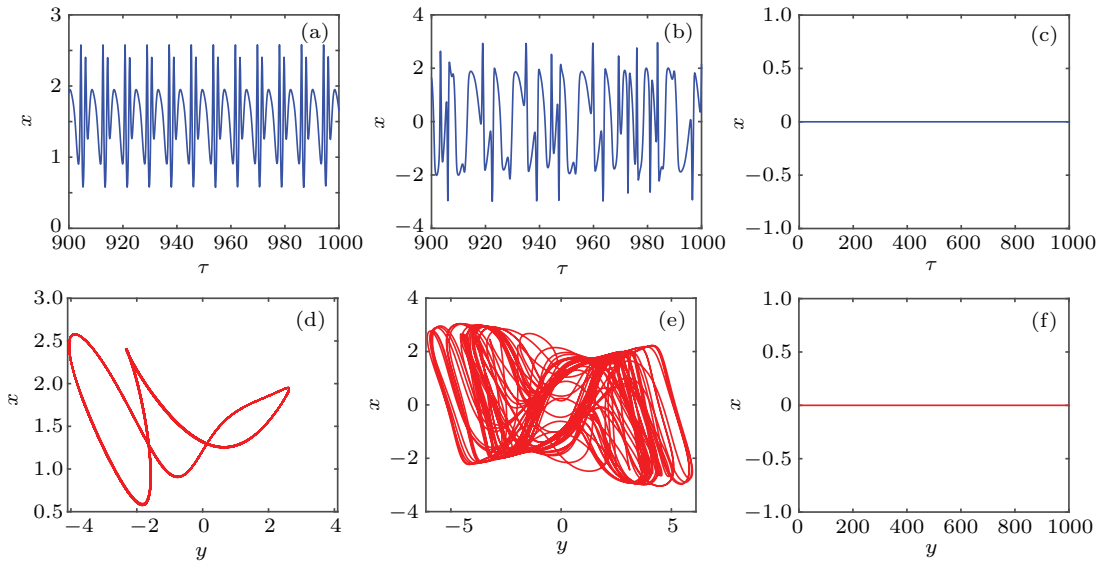


Fig. 3. The dynamical behavior of a memristive neural circuit. (a), (b) The time sequence and (d), (e) the corresponding y–x phase orbit when the initial value is (1.5, −0.2, 0.1, 0.2) and the parameter is selected at $\alpha = 1.0$ and 3.0, respectively. (c) The time sequence and (f) the corresponding y–x phase orbit are plotted when the initial value is (0, 0, 0, 0), while the other parameters are selected as $\beta = 0.71$ and $\eta = 0.01$.

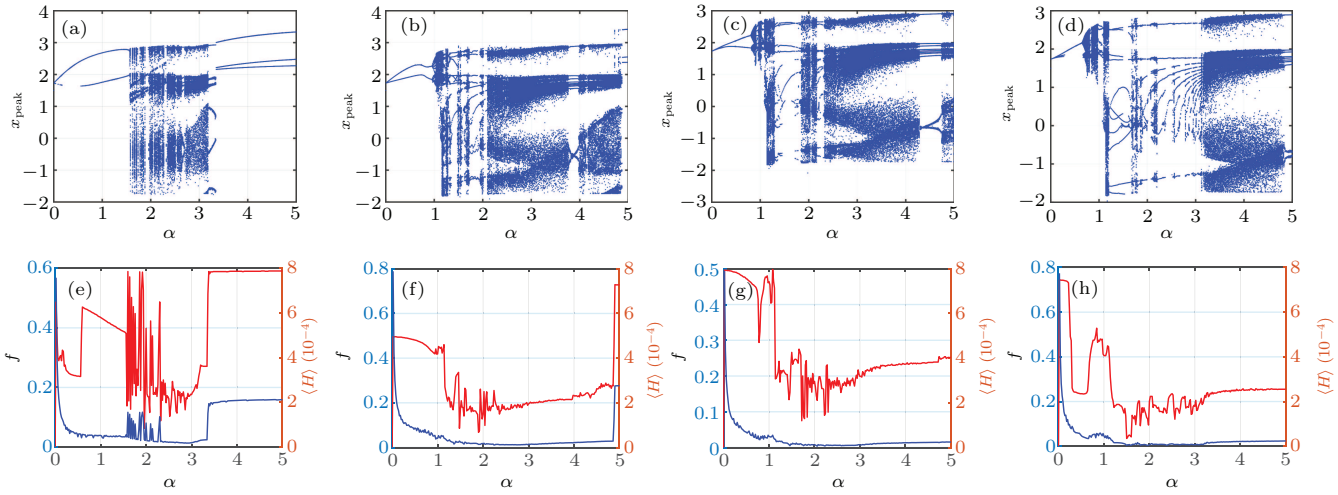


Fig. 4. The bifurcation diagram and energy change diagram for the memristive neural circuit with the increasing parameter α. (a)–(d) The peak value of x and (e)–(h) the corresponding energy change diagram when the parameter is selected at $\beta = 2.0$, 3.0, 3.5, and 4.0, respectively.

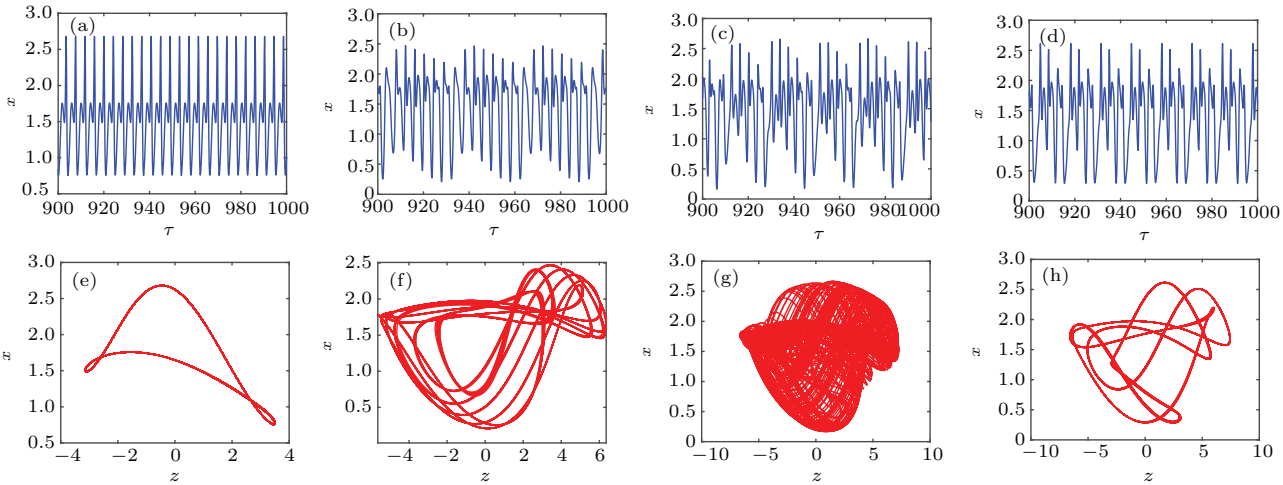


Fig. 5. The dynamical behavior of a memristive neural circuit. (a)–(d) The time sequence and (e)–(h) the corresponding z–x phase orbit when the parameter is selected at $\beta = 2.0$, 3.0, 3.5, and 4.0, respectively, while the other parameters are selected as $\alpha = 1.0$ and $\eta = 0.01$.

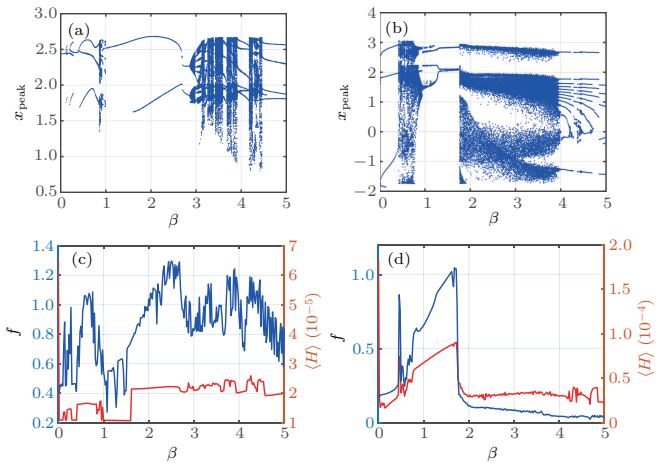


Fig. 6. The bifurcation diagram and energy change diagram for the whole system with the increasing parameter β. (a), (b) The peak value of x and (c), (d) the corresponding energy change diagram when the parameter is selected at $\alpha = 1.0$ and 3.0, respectively.

Figure 5 shows the dynamical behavior of the memristive neural circuit when changing the value of β while α and η are fixed as 1.0 and 0.01, respectively. To further investigate the effects of changes in parameter β on dynamical behavior, a bifurcation diagram and average energy change diagram for β are shown in Fig. 6 when another parameter α is fixed. Figures 6(a) and 6(b) respectively show the peak value of x when parameter β is modulated while $\alpha = 1.0$ and 3.0, respectively. It is found that the memristive neural circuit has multi-period firing patterns.

3.2. Synchronization of memristive neuronal network

The neural network is composed of the basic building blocks of neurons. The signal propagates within neurons coupling with electrical and chemical synapses. However, at the network level, information flowing or propagating among the intricately connected neurons still needs to be characterized. The memristive neuronal network is coupled by introducing the energy. We explore the dynamics of the network composed of 20 nodes by changing the coupling gain. The spatiotemporal dynamics and time series are depicted in Fig. 7.

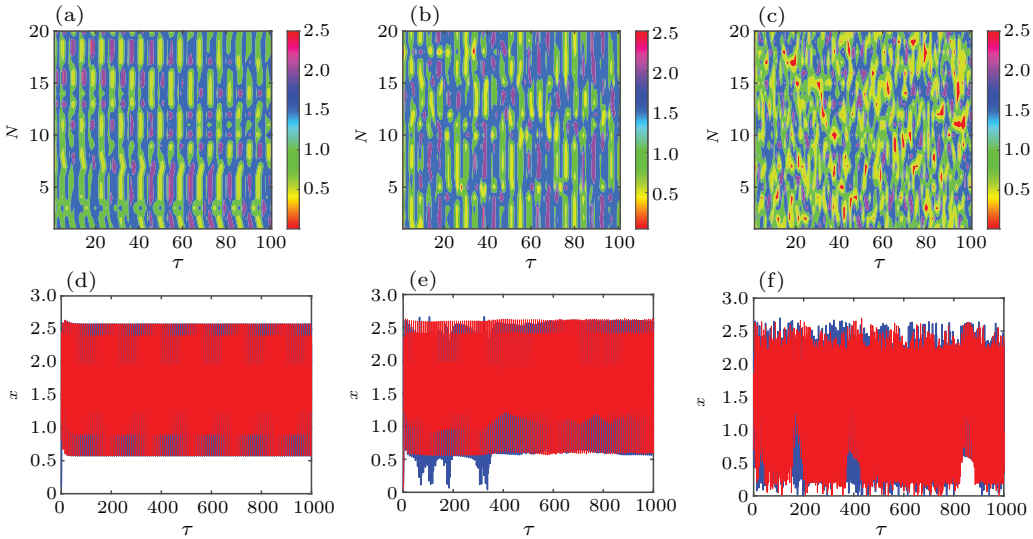


Fig. 7. The spatiotemporal patterns and time series of the memristive network with different values of parameter g_c. The parameter is selected at $g_c = 0.0$, 0.1, and 1.0, respectively, while the other parameters are set as $\alpha = 1.0$, $\beta = 0.71$, and $\theta = 0.0$.

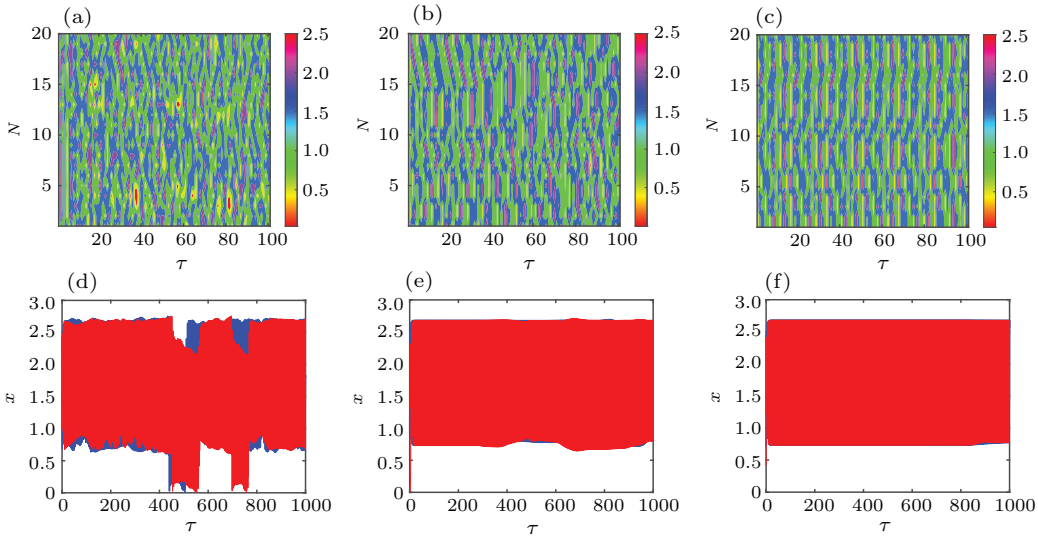


Fig. 8. The spatiotemporal patterns and time series of the memristive network with different values of parameter $\theta = 1$, 1000, and 3000, respectively, while the other parameters are controlled at $\alpha = 1.0$, $\beta = 2.0$, and $g_c = 0.2$.

Figure 7 shows that the spatiotemporal patterns are changed from synchronization into desynchronization in a network composed of memristive neural circuits under energy coupling. Almost all the models are periodically firing in Fig. 7(d), and the network presents a tidy pattern, as shown in Fig. 7(a). But the behavior of the network demonstrates irregular changes and chaotic evolution synchronously, when g_c increases to 0.1 and 1.0 in Figs. 7(b), 7(e) and 7(c), 7(f), respectively. Specifically, the network becomes desynchronized.

In Fig. 8, we investigate the synchronization dynamics in the network consisting of the memristive neural circuit by changing the values of θ while fixing the values of α, g_c, and β. In Fig. 8, it is demonstrated that under the modulation of θ, the network tends to be synchronized in Figs. 8(b) and 8(c). The nonlinear coupling successfully reconstructs the synchronization evolution of neural signals and also improves the understanding of the influence of single neurons on firing behavior. To process information effectively, coupling models associated with energy are well proposed, and memristive neurons tend to fire together in spontaneous activation when the stored energy in the coupling achieves a threshold. Based on the model associated with energy, the neural dynamical models are appropriate for depicting the complex and abundant firing spatiotemporal patterns.

4. Conclusion

Models of memristors are frequently used to construct neural circuits with firing patterns similar to biological neurons. Two capacitors and a memristor are connected to build a neural circuit. The neural circuit can characterize complex electromagnetic fields induced by bidirectional propagation and periodical exchange of ionic currents. By considering the controllability and flexibility of the cell membrane, the memristive system is employed to mimic its characteristics in neural circuits. The relationship between firing patterns and energy is identified by the Hamilton energy function. Further, the neuronal network is coupled by a new scheme associated with energy function. Identical neurons can reach synchronization at sufficiently large values of the coupling gain. This biophysical neuron with appropriate regulation of parameters is suitable for predicting and studying self-organization and energy balance in neural networks.

Acknowledgements

This study was funded by the National Natural Science Foundation of China (Grant No. 12302070) and the Ningxia Science and Technology Leading Talent Training Program (Grant No. 2022GKLRLX04).

References

[1] Friston K 2010 *Nat. Rev. Neurosci.* **11** 127
[2] Moujahid A, D'Anjou A, Torrealdea F J and Torrealdea F 2011 *Phys. Rev. E* **83** 031912
[3] Li S and Sheng Z H 2022 *Nat. Rev. Neurosci.* **23** 4
[4] Nowotny T and Rabinovich M I 2007 *Phys. Rev. Lett.* **98** 128106
[5] Canavier C C, Clark J W and Byrne J H 1990 *Biophys. J.* **57** 1245
[6] Rabinovich M I, Varona P, Selverston A I and Abarbanel H D I 2006 *Rev. Mod. Phys.* **78** 1213
[7] Hodgkin A L and Huxley A F 1952 *J. Physiol.* **117** 500
[8] Chua L, Sbitnev V and Kim H 2012 *Int. J. Bifurcat. Chaos* **22** 1230011
[9] Sah M P, Kim H and Chua L O 2014 *IEEE Circ. Syst. Mag.* **14** 12
[10] Lv M, Wang C N, Ren G D, Ma J and Song X L 2016 *Nonlinear Dyn.* **85** 1479
[11] Lv M and Ma J 2016 *Neurocomputing* **205** 375
[12] Bao H, Hu A H, Liu W B and Bao B C 2020 *IEEE T. Neur. Net. Lear.* **31** 502
[13] Ding S, Wang N, Bao H, Chen B, Wu H and Xu Q 2023 *Chaos Soliton. Fract.* **166** 112899
[14] Xie Y, Yao Z, Hu X K and Ma J 2021 *Chin. Phys. B* **30** 120510
[15] Zhang X F and Ma J 2021 *Journal of Zhejiang University: Science A* **22** 707
[16] Shen H, Yu F, Wang C H, Sun J R and Cai S 2022 *Nonlinear Dyn.* **110** 3807
[17] Wu F Q and Yao Z 2023 *Nonlinear Dyn.* **111** 13481
[18] Wu F Q, Guo Y T, Ma J and Jin W Y 2023 *Appl. Math. Comput.* **455** 128131
[19] Wu F Q, Guo Y T and Ma J 2022 *Nonlinear Dyn.* **109** 2063
[20] Zhang Y, Xu Y, Yao Z and Ma J 2020 *Nonlinear Dyn.* **102** 1849
[21] Wu F Q, Hu X K and Ma J 2022 *Appl. Math. Comput.* **432** 127366
[22] Guo Y, Wu F, Yang F and Ma J 2023 *Chaos* **33** 113106
[23] Xu Q, Ju Z, Ding S, Feng C, Chen M and Bao B C 2022 *Cogn. Neurodyn.* **16** 1221
[24] Zhang H, Wang L, Zhang P, Zhang X F and Ma J 2021 *Chin. Phys. B* **30** 038702
[25] Qiao S, Gao C H and An X L 2023 *Nonlinear Dyn.* **111** 10529
[26] An X L, Xiong L, Shi Q, Qiao S and Zhang L 2023 *Nonlinear Dyn.* **111** 9509
[27] Ma J and Tang J 2015 *Sci. China Technol. Sc.* **58** 2038
[28] Yang F F, Wang Y and Ma J 2023 *Commun. Nonlinear Sci.* **119** 107127
[29] Xie Y, Yao Z and Ma J 2022 *Front. Inform. Technol. Electron. Eng.* **23** 1407
[30] Ma J 2024 *Appl. Math. Comput.* **463** 128379
[31] Xie Y, Zhou P and Ma J 2023 *Appl. Math. Model.* **113** 175
[32] Xie Y, Zhou P, Yao Z and Ma J 2022 *Physica A* **607** 128175
[33] Torrealdea F J, D'Anjou A, Graña M and Sarasola C 2006 *Phys. Rev. E* **74** 011905
[34] Liu Z L, Yu Y and Wang Q Y 2022 *Sci. China Technol. Sc.* **65** 1435
[35] Liu Z, Han F and Wang Q Y 2022 *Nonlinear Dyn.* **108** 1849
[36] Torrealdea F J, Sarasola C and d'Anjou A 2009 *Chaos Soliton. Fract.* **40** 60
[37] Wu F Q and Wang R B 2023 *Commun. Nonlinear Sci.* **126** 107459
[38] Zhou P, Zhang X F and Ma J 2022 *Nonlinear Dyn.* **108** 1681
[39] Wu F Q, Ma J and Zhang G 2020 *Sci. China Technol. Sc.* **63** 625
[40] Xie Y, Xu Y and Ma J 2023 *Nonlinear Dyn.* **111** 11521
[41] Xie Y and Ma J 2022 *J. Biol. Phys.* **48** 339
[42] Xie Y, Yao Z and Ma J 2023 *Sci. China Technol. Sc.* **66** 439
[43] Yang Z, Zhang Y and Wu F Q 2020 *Nonlinear Dyn.* **100** 647
[44] Usha K and Subha P A 2019 *Chin. Phys. B* **28** 020502
[45] Malik S A and Mir A H 2020 *Neural Networks* **123** 372
[46] Herz A V M, Gollisch T, Machens C K and Jaeger D 2006 *Science* **314** 80
[47] Wu F Q, Meng H and Ma J 2024 *Neural Networks* **169** 607
[48] Barry J F, Turner M J, Schloss J M, Glenn D R, Song Y, Lukin M D, Park H and Walsworth R L 2016 *Proc. Natl. Acad. Sci. USA* **113** 14133
[49] Chua L O 1971 *IEEE T. Circ. Theory* **18** 507
[50] Song X L, Jin W Y and Ma J 2015 *Chin. Phys. B* **24** 128710
[51] Sarasola C, Torrealdea F J, D'Anjou A, Moujahid A and Graña M 2004 *Phys. Rev. E* **69** 011606
[52] Heitmann S, Aburn M J and Breakspear M 2018 *Neurocomputing* **315** 82